the plunger position closest to the input terminal, and assigning any additional losses to the moving element.[9]

ACKNOWLEDGMENT

The author wishes to thank B. C. Yates and J. F. LaBrecque for their constructive suggestions in the preparation of this manuscript.

REFERENCES

[1] A. L. Cullen, "Measurement of microwave transmission efficiency," *Wireless Eng.*, vol. 26, pp. 255–258, Aug. 1950.
[2] R. W. Beatty, G. F. Engen, and W. J. Anson, "Measurement of reflections and losses of waveguide joints and connectors using microwave reflectometer techniques," *IRE Trans. Instrum.*, vol. I-9, pp. 219–226, Sept. 1960.
[3] G. Almassy, "A first-order correction to sliding short behavior with application to the problem of measuring small losses," *IEEE Trans. Instrum. Meas.*, vol. IM-20, pp. 162–169, Aug. 1971.
[4] G. F. Engen, "An extension to the sliding short method of connector and adapter evaluation," *J. Res. Nat. Bur. Stand.*, vol. 75C, pp. 177–183, July–Dec. 1971.
[5] N. T. Larsen and F. R. Clague, "The NBS type II power measurement system," presented at the 1970 Instrumentation Society of America Meeting, Philadelphia, Pa., Oct. 26–29, 1970, Paper 712-70.
[6] E. L. Komarek and P. V. Tryon, "An application of the power equation concept and automation techniques to precision bolometer unit calibration," *IEEE Trans. Microwave Theory Tech.*, this issue, pp. 1260–1267.
[7] G. F. Engen, "Theory of UHF and microwave measurements using the power equation concept," Nat. Bureau Standards, Boulder, Colo., Tech. Note 637.
[8] I. Kasa, "Exact solution of network analyzer calibration and two-port measurements by sliding terminations," presented at the 1974 Conf. Precision Electromagnetic Measurements, London, England.
[9] ——, private communication.
[10] D. M. Kerns and R. W. Beatty, *Basic Theory of Waveguide Junctions and Introductory Microwave Network Analysis*. New York: Pergamon, 1967.

[9] While a rigorous proof of this statement would be lengthy, it is perhaps intuitively plausible, and in any event has been demonstrated on the computer.

An Application of the Power Equation Concept and Automation Techniques to Precision Bolometer Unit Calibration

ERNEST L. KOMAREK, MEMBER, IEEE, AND PETER V. TRYON

Abstract—**The power equation concept has been implemented into a multioctave precision bolometer unit calibration system employing automation techniques in conjunction with an automatic network analyzer (ANA) system. Using statistical methods the system is being evaluated as a calibration transfer system operating in the 2–12.4-GHz frequency range at 1–10 mW. Preliminary results reported here show a single measurement standard deviation of 0.2–1 percent from 2–10 GHz. Upon a successful evaluation, the system will be qualified as an integral part of the national measurement system.**

INTRODUCTION

THE NEED for multiple frequency calibration services has been served by the combination of the power equation concept [1] with an automated network analyzer (ANA) in the development of a multioctave bolometer unit calibration system. The system is capable of measuring the effective efficiency of coaxial and waveguide type bolometer units at 100-MHz intervals in the 2–12.4-GHz frequency range at power levels of 1–10 mW.

The core of the system is an optimal configuration of broad-band directional couplers which form a 4-port network (see Fig. 1) and the use of power equation concepts to describe the transfer of RF power between a source and a load. The ANA facilitates the measurement of complex voltage ratios which are required for the evaluation of mismatch factors and terms which are related to the 4-port network and the ANA measurement system.

Techniques consistent with the requirements of precision measurement practices were developed for the calibration of the system over its entire frequency range. Statistical methods were then applied in this initial evaluation of systematic and random sources of error, and for the collection of control chart data.

This paper describes the evaluation of a specific type of systematic error and the initial estimation of total

Manuscript received May 21, 1974; revised August 30, 1974.
E. L. Komarek is with the RF Power, Current and Voltage Section, Electromagnetics Division, Institute for Basic Standards, National Bureau of Standards, Boulder, Colo. 80302.
P. V. Tryon is with the Statistical Engineering Laboratory, National Bureau of Standards, Boulder, Colo. 80302.

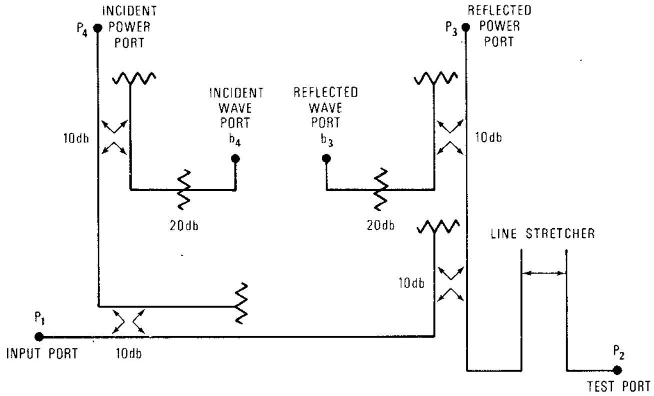

Fig. 1. 4-port directional coupler.

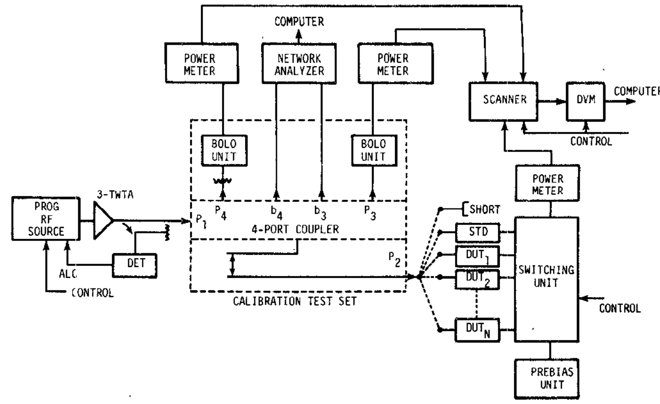

Fig. 2. Bolometer unit calibration system block diagram.

random error. Some mention is made of additional evaluation in progress but detailed results will be given later.

THEORETICAL BACKGROUND AND INSTRUMENTATION

A brief review of the application of the power equation concept by others [2], [3] to microwave power measurements may be in order. A calibrated power generator or a standard power meter using the substitution principle is commonly used for the calibration of power meters. The equation that provides the ratio of the power delivered to the unknown and the standard power meters, P_{gu} and P_{gs}, respectively, is

$$P_{gu} = P_{gs} \frac{|1 - \Gamma_g \Gamma_s|^2 (1 - |\Gamma_u|^2)}{|1 - \Gamma_g \Gamma_u|^2 (1 - |\Gamma_s|^2)} \tag{1}$$

where Γ_g is the generator reflection coefficient, and Γ_u and Γ_s are the reflection coefficients of the unknown and standard, respectively.

In the case of bolometric type power meters, the ratios of effective efficiencies of the unknown and standard bolometer units, η_u and η_s, respectively, the equation may be written as

$$\eta_u = \eta_s \frac{P_{bu} |1 - \Gamma_g \Gamma_u|^2 (1 - |\Gamma_s|^2)}{P_{bs} |1 - \Gamma_g \Gamma_s|^2 (1 - |\Gamma_u|^2)} \tag{2}$$

where P_{bu} and P_{bs} are, respectively, the bolometrically substituted dc powers in the unknown and standard bolometer units. By use of the power equation

$$P_{gl} = M_{gl} P_g \tag{3}$$

where P_{gl} is the net power delivered by the source to a load, P_g is the available power from that source, and M_{gl} is the mismatch factor which describes the conditions for power transfer from the source to the load. The term M_{gl} is a real number and does not require manipulation of complex numbers for its evaluation.

Equation (2) is greatly simplified by the application of (3) as

$$\eta_u = \eta_s \frac{P_{bu} M_{gs}}{P_{bs} M_{gu}} \tag{4}$$

and does not require the individual measurement of the reflection coefficients Γ_g, Γ_u, and Γ_s. Instead, the M_g are evaluated by

$$M_{gl} = 1 - \frac{|W_l - R_c|^2}{R^2} \tag{5}$$

where R and R_c are properties of a 4-port network and the measuring system and W_l represents the response of the measurement system with the load connected to the 4-port.

The configuration, Fig. 1, of multioctave coaxial directional couplers allows the measurement of the complex voltage ratio b_3/b_4 which is needed for the evaluation of R, R_c, and W_l. The power measurement of P_4 accounts for variations in power level during various phases in the overall substitution and measurement process. The line stretcher facilitates adjustment of the reference and signal transmission lines to equal physical and electrical length and also provides a sliding short function during the calibration process.

The block diagram shown in Fig. 2 represents the calibration transfer system which is integrated with a commercial ANA which normally operates in the frequency range of 100 MHz–18 GHz. It includes system components such as the prebias and switching units which facilitate the handling of up to 16 bolometer units, power meters for monitoring the incident power to the test set P_4, and the reflected power P_3. The latter is used during applications [4] of the test set other than bolometer unit calibration. Additional auxiliary equipment includes three traveling-wave-tube amplifiers for the coverage of the 2–12.4-GHz range with adequate power input to the test set so that up to 10 mW of microwave power is available at the test port.

CALIBRATION AND MEASUREMENT PROCESS

Calibration of the system is accomplished in two phases, the evaluation of R and R_c, and the measurement of RF power at the test port P_2 relative to the power at P_4 using a previously calibrated working standard. The measurement of the latter is quite straightforward; however, the evaluation of R and R_c required the development of the technique described in the following.

With a short circuit connected to the test port the complex ratio b_3/b_4 describes a circle in the complex plane as the line stretcher position is changed. Due to losses in the line stretcher, the locus of points in the complex plane is an approximation to a circle, as compared to the use of sliding short for calibration purposes. However, the failure of the line stretcher to be ideal causes only a second order error in the final measurement results. This circle, having radius R and center R_c, is not necessarily centered at the origin. At each programmed frequency the network analyzer measures b_3/b_4 for each position of the line stretcher. The computer program has been designed to accommodate up to 15 measurements, and to least squares fit the data to a circle and determine its radius and center. These data are stored for later determination of M_{gs} and M_{gu}. The tests described in the following are included in the computer program to assure the operator of a valid calibration.

Fig. 3 is a typical printout of the circle fitting results. At each frequency the radius of the fitted circle R is tabulated in the column under "Radius," while the X and Y coordinates of the center of the circle are shown under "XCEN" and "YCEN," respectively. The "Residual" column shows the deviation, along the radius, of the measured points from the fitted circle for each measurement position of the line stretcher. The final entry at each frequency in this column is the root mean square of the residuals in percent. The effect of the data point distribution around the circle was investigated by Kasa [5] and a routine for the verification of an adequate distribution of points was developed to aid the operator with the system calibration process. This routine compares the area of an inscribed polygon determined by the data points with the area of a regular inscribed polygon of an equal number of points. This ratio, shown in the "Area" column of Fig. 3, is used by the operator to verify a valid system calibration for the number of data points used and their distribution.

The system calibration process is completed with the evaluation of M_{gs} and the system factor

$$K_A = \left(\eta_s \frac{P_{b4s}}{P_{bs}} M_{gs}\right)^{-1} \qquad (6)$$

where P_{b4s} represents the bolometrically substituted dc power at P_4 of the 4-port network with the working standard connected to the test port, and M_{gs} evaluated by (5). Fig. 4(a) illustrates a typical printout of the calibra-

FREQUENCY	AREA	RADIUS	XCEN	YCEN	RESIDUAL
4000	.87	2.5634	.149034	.015004	-.24E-01
					-.32E-02
					.720E-02
					-.22E-01
					.128E-01
					-.74E-03
					.208E-01
					-.10E-01
					.594E-02
					.127E-01
					.552E+00%
4200.	.86	2.5541	-.04450	-.07868	-.19E-01
					-.29E-02
					.465E-02
					-.15E-01
					.840E-02
					.156E-02
					.197E-01
					-.14E-01
					.960E-02
					.676E-02
					.467E+00%
4400.	.93	2.5178	.028729	054846	-.12E-01
					-.14E-01
					.320E-02
					-.13E-01
					.806E-02
					-.14E-02
					.218E-01
					-.19E-01
					.167E-01
					.945E-02
					.532E+00%
4600.	95	2.5151	.029879	.014239	- 50E-02
					-.16E-01
					-.25E-02
					-.76E-02
					.640E-02
					-.74E-03
					210E-01
					-.12E-01
					.154E-01
					.691E-02
					470E+00%

Fig. 3. Typical system calibration printout.

STD. NO -- 2209 ID--STANDARD

FREQUENCY	KA	MGL	PMAIN	PSIDE
4000	1 60880	98850	7.4225	4.7452
4200.	1 58169	.99565	7.4782	4 8290
4400.	1.56509	99663	8.1854	5.3420
4600.	1 56504	99752	8.8199	5.8077
4800.	1.54991	.99253	8.0690	5.3474
5000.	1.53589	99905	7.4391	4.9456
5200	1 51527	99352	7.6209	5 1671
5400	1.50310	.99898	8 6738	5 8900
5600	1.49137	99968	9.9281	6.8034
5800	1.48588	.98945	10.6779	7 4210
6000	1 47306	98749	10 3040	7 2378
6200	1 46112	99882	9 5071	6.6902
6400	1 44296	98482	8 9367	6 4315
6600.	1 43368	98258	8 5117	6 1832
6800.	1 42116	.99233	9 1453	6.6095
7000	1 40597	99829	10 0577	7.3296
7200.	1 40447	.99391	10 0489	7 3757
7400	1.39804	99747	9 5328	7 0194
7600	1.38257	99917	8 5324	6 3769
7800	1.39110	97929	7 5258	5 6690
8000	1.39554	.99176	7 3931	5 4767

(a)

UNKNOWN NO.-- 2280 ID--UNKNOWN

FREQUENCY	EFFICIENCY	MGL
4000	.97914	.99938
4200	.97905	99504
4400	.97874	.99712
4600	97851	.99792
4800	97813	99345
5000	97798	.99928
5200	.97778	99438
5400.	97691	99882
5600	97654	99044
5800.	97571	.99090
6000	.97614	98741
6200	97588	99916
6400	.97517	98528
6600	97479	98231
6800	97447	99332
7000	97365	99783
7200	97352	.99379
7400.	97339	.99692
7600	97342	.99834
7800	97360	.97792
8000.	97373	99124

(b)

Fig. 4. (a) Typical test port calibration printout. (b) Typical bolometer unit calibration printout.

tion results including both the test port power level ("PMAIN") and P_4 ("PSIDE").

The calibration of an unknown bolometer unit is accomplished by: 1) the substitution of the working standard for the unknown, 2) the measurement of P_{b4u} and P_{bu}, and 3) the evaluation of M_{gu}. Then the effective efficiency of the bolometer unit is

$$\eta_u = \frac{P_{bu}}{P_{b4u}} \frac{1}{M_{gu}} \frac{1}{K_A}$$

$$= \eta_s \frac{P_{bu}}{P_{bs}} \frac{M_{gs}}{M_{gu}} \frac{P_{b4s}}{P_{b4u}} \tag{7}$$

where P_{b4u} represents the bolometrically substituted dc power at P_4, and the ratio P_{b4s}/P_{b4u} serves to account for power variation during the bolometer unit substitution process. Fig. 4(b) illustrates typical printouts of the final measurement results.

MEASUREMENT ERROR EVALUATION

The usual approach to measurement error evaluation is to separate the measurement system into its critical subsystems, evaluate the potential for systematic error in each (theoretically or experimentally), and by application of error propagation procedures determine the effect on the final measurement result. However, with a system as complex as described earlier, this approach was determined to be impractical. Therefore, a more direct approach employing modern statistical methods for the evaluation of both systematic and random errors was chosen.

For statistical evaluation it is necessary to consider the actual measurement as the ratio of two unknown effective efficiencies:

$$\frac{\eta_u}{\eta_s} = \frac{P_{bu} M_{gs} P_{b4s}}{P_{bs} M_{gu} P_{b4u}}. \tag{8}$$

Equation (8) can be considered to be ideal only to the extent that all the measured quantities on the right can be determined without error. However, if the presence of measurement errors is recognized, a statistical model can be written as

$$y = \frac{\eta_u}{\eta_s} + e \tag{9}$$

where y is the measured value of the ratio, η_u and η_s are the true values of the effective efficiencies of the bolometer units, and e is the measurement error resulting from the combined effects of the four powers and two mismatch factor measurements.

The measurement errors are characterized by a probability distribution whose variance and shape are affected by the random errors from one measurement to the next, and by day-to-day variations. The former source of errors is attributable to short term sources of variance, e.g., connector nonrepeatability and instabilities in system components, while the day-to-day or "occasion-to-occasion" errors are due to subtle variations in the system setup, calibration, RF signal switching nonrepeatability, etc. The effect of systematic errors which remain constant for relatively long periods of time is a shift in the mean of the error distribution away from zero. Other sources of error must be classified somewhere between random and systematic. For example, an annual cyclic error might be introduced by room temperature and/or humidity changes due to the pattern of air conditioning use over the year while systematic error can "appear" (or even disappear) when the system undergoes periodic maintenance or a new operator is employed. The latter sources of error are easily uncovered by proper collection of system surveillance data and use of control charts. The latter was not of concern during the initial evaluation; however, the collection of data for this purpose was started at that time.

The occasion-to-occasion sources of error of the calibration transfer system are of particular importance; since the ANA system is also used for other measurement functions. This results in a "new" and independent system setup each time the system is switched into the bolometer unit calibration mode. The total random error standard deviation reported in this paper includes the effects of occasion-to-occasion error. Additional experimentation is in progress to separate the components of random error within and between occasions. This is necessary for the assignment of estimates of uncertainty in a calibration procedure. The standard deviation of bolometer unit measurements from a calibration procedure will be different from the single measurement standard deviation described here. However, it will be of the same order of magnitude or smaller.

From (9) it is evident that the basic measurement made by the system is the ratio of effective efficiencies of two bolometer units. In practice, η_s the effective efficiency of the working standard, is known as a result of previous evaluation relating to a National Bureau of Standards reference standard. Therefore, the desired result η_u, the effective efficiency of the unknown, is computed from

$$\eta_u = y \cdot \eta_s. \tag{10}$$

Systematic errors can arise in four ways as follows.

1) Error in effective efficiency η_s of the working standard.

2) Error caused by the measurement system only and not the working standard or unknown bolometer units.

3) Error caused by an interaction between the system and the working standard.

4) Error caused by an interaction between the system and the unknown bolometer unit being measured.

The first type of systematic error is not a function of the transfer system being evaluated but is a function of the evaluation of the working standard relative to the primary reference standard. The error associated with the primary standard is determined at that time and therefore does not enter into this discussion.

In the case where a systematic error Δ of the second type is present the measured ratio is

$$y = \frac{\eta_u}{\eta_s} + \Delta + e \quad (11)$$

where e is a zero mean random error. Since Δ is not a function of the bolometer units referred to as standard and unknown, their roles can be interchanged and as in (10) the measured ratio becomes

$$y' = \frac{\eta_s}{\eta_u} + \Delta + e' \quad (12)$$

where Δ is acting in the same direction as in (10). Forming a product of (10) and (11) yields

$$yy' = 1 + \left(\frac{\eta_s}{\eta_u} + \frac{\eta_u}{\eta_s}\right) \Delta + \Delta^2 + e^* \simeq 1 + 2\Delta + e^* \quad (13)$$

where e^* is a random error term, and the presence of a nonzero Δ is determinable by obtaining a random sample of yy' products over a period of time using a variety of bolometer units.

The type 3 and 4 systematic errors are of the same nature since both the working standards and unknowns are bolometer units. However, the consequences are quite different. The type 3 error occurs with the working standard and thus results in a systematic error for all calibrations, while the type 4 error occurs with the unknown and emerges in a random manner with respect to the population of all bolometer units calibrated but in a systematic manner for repeated measurements of a single bolometer unit.

Errors of type 3 and 4 do not yield to evaluation as the second type because inverting the ratio also inverts or reverses the direction of the bias. Other techniques are being developed to evaluate these types of error; however, as long as the bolometer units are of a like type, it seems unlikely they would interact differently; and, furthermore, like interactions will cancel in the measured ratio.

DESIGN OF THE RATIO EXPERIMENT

The ratio experiment was the first of two exercises designed to evaluate the bolometer unit calibration system attached to the ANA. The primary objective of the ratio experiment was to evaluate the type of systematic error discussed earlier. In addition, information on total random errors and on practical operation of the system were valuable by-products of the experiment. The second experiment, mentioned here only for completeness, was designed to accommodate an ongoing calibration work load by simulating normal operation for the purpose of estimating the random errors (particularly occasion-to-occasion errors) of the process and to obtain initial data for control charts and other quality control procedures.

Five bolometer units, A–E, with type N connectors were chosen to represent a variety of bolometer unit properties. Two units are "normal" (A and D), one high VSWR (B), one low effective efficiency (C), and E has a frequency response which is different from the four units.

The experiment was conducted on ten separate occasions in each of three frequency bands at which the system normally operates, i.e., 2–4, 4–8, and 8–12.4 GHz. Each frequency band was treated separately because different equipment is involved in each band, e.g., these are normal operating frequency ranges of the traveling-wave-tube amplifiers and signal sources employed in the system. For each occasion the ratios of the ten possible pairs of bolometer units were measured. On five randomly chosen occasions the ratios were in one direction and on the remaining occasions the inverses were measured. This reversal in the measurement order of the bolometer unit pairs was done to form the yy' products used in (13).

These ratios were measured at 40 randomly ordered frequency points in each of the three frequency bands. Two randomly selected frequency sequences were employed alternately between occasions. Thus data were obtained on 10 occasions for 50 products of ratios (5 occasion pairs times 10 bolometer unit combinations) at each of 120 frequencies in the 2–12.4-GHz frequency range.

On each measurement occasion the system was calibrated just prior to the measurement of the ratios η_u/η_s and the M_{gl} for each bolometer unit. In addition to the ratio and M_{gl} measurements, the M_{gl} of the short used in the system calibration was measured after the fifth and tenth bolometer unit pairs. The latter allowed a study of the calibration stability of the system.

DATA ANALYSIS

A first attempt at the statistical analysis revealed a number of extreme outliers or abnormal measurements. In cases where the system operators had noted abnormal system behavior and had repeated the measurements, the second set of data were used in the final analysis. The remaining extreme outliers were omitted from the analysis. This action seems justifiable since the outliers were so extreme that they would normally be detected by control charts. A second pass at the statistical analysis showed that about 3 percent of the remaining measurements appeared as outliers in the sense that the measurement errors were much larger than was characteristic of the remaining 97 percent. These unexplained outliers were retained in the data to avoid concealing a real part of the random error mechanism of the measurement process.

The 100 ratio measurements at each frequency were analyzed using an OMNITAB [6] program. Four major outputs included the following.

1) Least squares estimates of the ratios η_B/η_A, η_C/η_A, η_D/η_A, η_E/η_A, their standard deviations, the residual errors, and the residual standard deviations.

2) Plots and tests of randomness of the residual errors.

3) Plots and one way analysis of the residuals grouped by occasion and also grouped by bolometer unit pair.

4) The 50 products of inverse ratios, plots of them versus frequency and bolometer unit pairs, and a statistical analysis of them.

Fig. 5 shows plots of the effective efficiency of bolometer units B–E relative to the effective efficiency of bolometer unit A. The pair of lines at the bottom of the figure shows the width of a 95-percent confidence interval for the true ratio at each frequency. Variations in the effective efficiency ratio curves of an amplitude equal to the width of the confidence interval can be attributed to random errors in the experiment while larger amplitude variations can be considered real.

Bolometer units A and D are of similar types and are known to have effective efficiencies varying smoothly from about 0.98 at 2 GHz to 0.96 at 12 GHz. This close match seems to be verified by the curve labeled η_D/η_A in Fig. 5; furthermore, examination of the other curves reveals that none of the sharp variations are common to all and thus are not caused by the frequency response of bolometer A. It should be kept in mind that the plots differ from plots of the bolometer unit effective efficiency only by a multiplicative constant which varies from about 1.02 at 2 GHz to 1.04 at 12 GHz (the reciprocal of the effective efficiency of bolometer unit A). It follows that the sharp variations of bolometer units B and C in the 10–12-GHz region and the "spike" at 7 GHz for bolometer unit E are either real properties of these units or the result of a type 4 systematic error. In general the slower downward trends in effective efficiency as a function of frequency are known to be real properties of bolometer units.

The residual standard deviation is an estimate of the standard deviation of a single measurement. These are shown in Fig. 6 and contain the effect of both within and occasion-to-occasion random error. Note that three separate systems are represented in the frequency ranges: 2–4, 4–8, and 8–12 GHz. In each range the precision is characterized by a "baseline" curving upwards with frequency. The sharp spikes are caused by "bad" occasions. Typically, the precision on 1–3 of the ten occasions was extremely bad (but perfectly normal at an adjacent frequency), while the remaining occasions were normal. (This was later determined to be an intermittent malfunction of the ANA which was corrected for subsequent experiments.) The remaining "normal" occasions were used to estimate the "usual" precision. This is shown by dots below the peaks in the solid curve of Fig. 6. However, the major peak between 11 and 11.7 GHz was produced by consistently bad precision on all occasions. This was later identified as a system malfunction and its correction will be verified during future experiments.

The baseline values shown in Fig. 6 are reasonable measures of precision of the measurement process since control chart procedures are used to detect "bad" occasions. The standard deviation of a single measurement ranges from 0.2 percent at 2 GHz to 1 percent at 12 GHz except between 11 and 11.7 GHz. The increase in standard deviation at higher frequencies is believed to be caused by nonrepeatable losses associated with the connectors.

Plots of the mean and 25-percent trimmed mean of the 50 products of pairs of inverse ratio measurements (13) at each frequency are shown in Fig. 7. Recall that in the absence of measurement error each product would be 1.0. Of course, random errors are present, but in the absence of a systematic error of type 2, the average of the set of 50 should not be (statistically) significantly different from 1.0. The figures clearly show that this is not so and a systematic error is present.

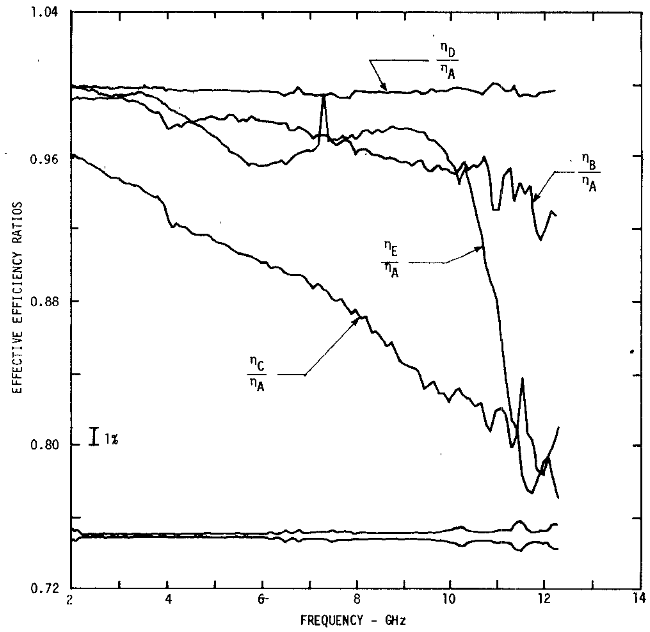

Fig. 5. Effective efficiency ratios of bolometer unit pairs.

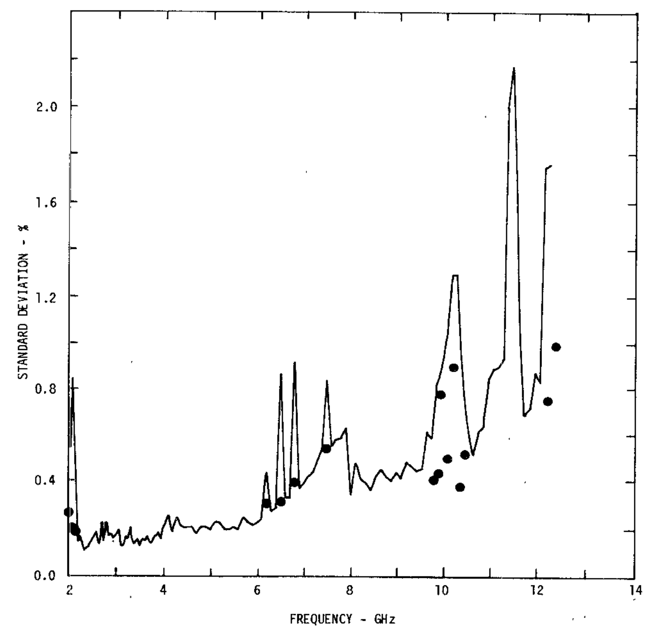

Fig. 6. Standard deviation for a single measurement.

The 25-percent trimmed mean is computed by ignoring the 25-percent largest and smallest observations and averaging the middle 50 percent. This technique eliminates the effect of "outliers" and gives, in this case, a better estimate of the "center" of the distribution. When the observations that are ignored are symmetrical above and

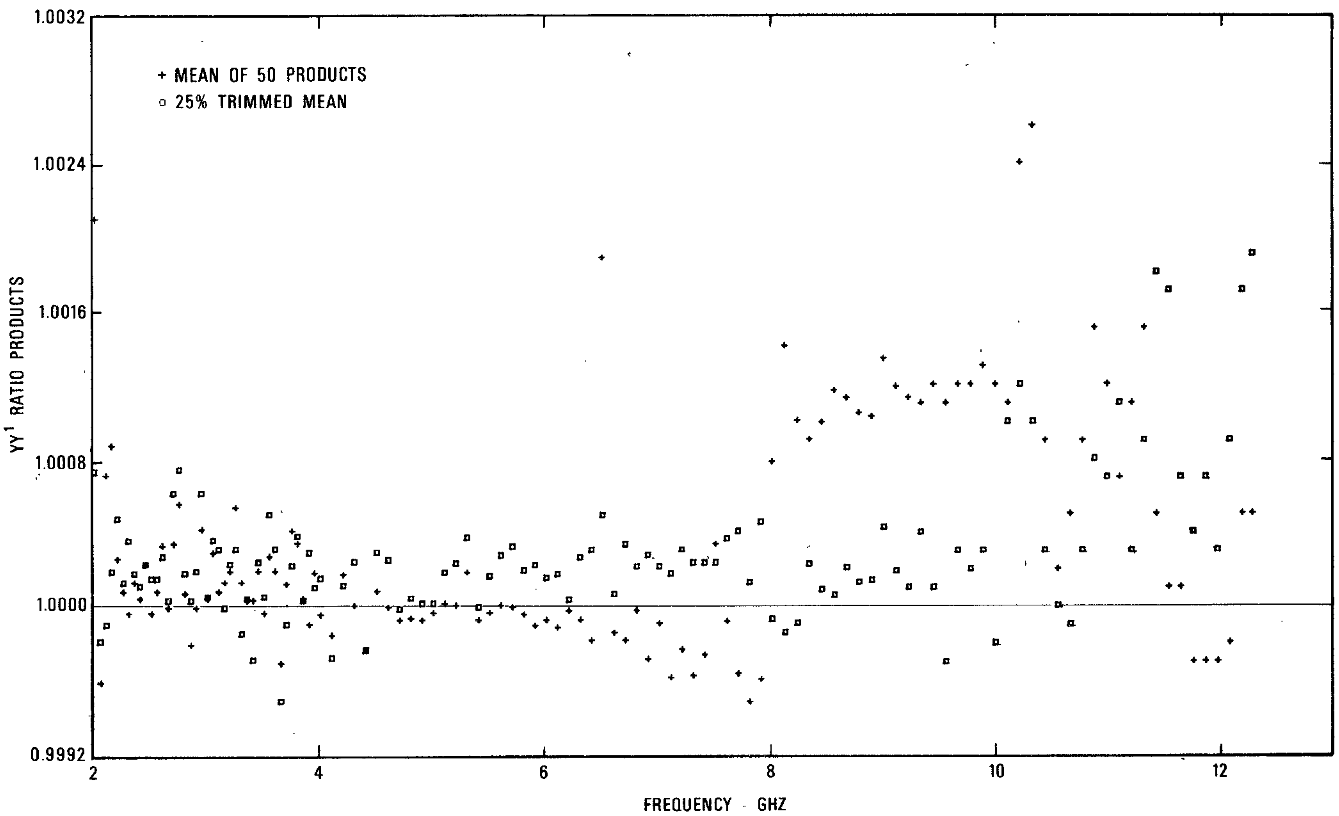

Fig. 7. Plots of mean and 25-percent trimmed mean of 50 products of pairs of inverse ratios.

below the mean, the trimmed mean and usual mean or average tend to be very close, e.g., in the 2–4-GHz range. On the other hand, when observations are asymmetrical, the mean and trimmed mean differ greatly, e.g., 8–12 GHz.

The plots clearly show that the characteristics of the three "systems" (frequency bands) are different. In the 2–4-GHz range the distribution products are symmetric with a systematic error averaging +0.0002 (0.02 percent) and bounded by +0.04 percent. From 4–8 GHz the trimmed mean indicates a positive systematic error of the same magnitude as in the 2–4-GHz band. However, the asymmetry indicates "outliers" on the low side. The 8–12.4-GHz range must be considered in two parts. From 8–10 GHz the trimmed mean indicates the same positive systematic error as at lower frequencies, but outliers are now predominantly high. Above 10 GHz a positive systematic error is evident but poorer precision makes other conclusions difficult.

Clearly, the design of the experiment has the sensitivity to resolve very small type 2 systematic errors, and that systematic errors of this type do exist. However, they are negligible in comparison to random errors (0.2–1 percent) and type 1 systematic errors which will be on the order of 1–2 percent.

On each occasion each bolometer unit was attached to the test port four times and its M_{gl} was obtained in the course of the measurement. The M_{gl} for each bolometer connection was so good that composite plots of the four connections on one occasion appear as a single line with few exceptions. This indicates that within occasion random error due to repeated connection is very small. Although this seems inconsistent with other random error observations attributed to connector repeatability, it suggests that connector nonrepeatability is due to changes in the efficiency factor (dissipative loss) of each connection and not an impedance discontinuity.

CONCLUSIONS

The power equation concept and the automatic techniques were implemented into an automated bolometer unit calibration system in the frequency range of 2–12.4 GHz at 1–10-mW power level. The preliminary evaluations show total random error standard deviation of a measurement range from 0.2 to 1 percent over the frequency range. Experimental procedures for evaluating one type of systematic error showed that it could be neglected. As an additional benefit the statistical procedures used were helpful in detecting system malfunctions which then could be corrected. Additional experimentation is being analyzed and future experimentation is planned to complete the evaluation for qualification of the system as an integral part of the national measurement system. Additional evaluation is necessary in the 10–12.4-GHz range to verify the correction of a system malfunction and to determine the precision in this range.

ACKNOWLEDGMENT

The authors wish to thank Dr. G. F. Engen for technical guidance and assistance. They also wish to thank M. P. Weidman, who provided the computer programs for the system control and measurement process; J. Donaldson, who analyzed and summarized the results; and G. L. Rosenberger, who assisted with the data collection and processing. The authors greatly appreciated all their efforts.

REFERENCES

[1] G. F. Engen, "An introduction to the evaluation of microwave systems using terminal invariant parameters," Nat. Bureau Standards, U. S. Dep. Commerce, Boulder, Colo., NBS Monogram 112, Oct. 1969.
[2] F. R. Hume, F. K. Koide, and D. J. Dederich, "Practical and precise means of microwave power meter calibration transfer," *IEEE Trans. Instrum. Meas.* (*1972 Conference on Precision Electromagnetic Measurements*), vol. IM-21, pp. 457–466, Nov. 1972.
[3] G. F. Engen, "Theory of UHF and microwave measurement using the power equation concept," Nat. Bureau Standards, U. S. Dep. Commerce, Boulder, Colo., NBS Tech. Note 637, Apr. 1973.
[4] ——, "Calibration technique for automated network analyzers with application to adapter evaluation," this issue, pp. 1255–1260.
[5] I. Kasa, "Error analysis of a circle fitting procedure," Nat. Bureau Standards, U. S. Dep. Commerce, Boulder, Colo., to be published.
[6] D. Hogben, S. T. Peavy, and R. N. Varner, "OMNITAB II user's reference manual," Nat. Bureau Standards, U. S. Dep. Commerce, Boulder, Colo., NBS Tech. Note 552, Oct. 1971.

A Microwave Dosimetry System for Measured Sampled Integral-Dose Rate

CHRISTOPHER L. CHRISTMAN, MEMBER, IEEE, HENRY S. HO, MEMBER, IEEE, AND SHEPPARD YARROW

Abstract—**An interface has been developed to allow the measurement of sampled integral-dose rate, defined as the change in integral dose during a particular time interval divided by that interval, absorbed by test animals as they are exposed in a waveguide to 2450-MHz CW microwave energy. The purpose of this investigation is to quantify the variations in sampled integral-dose rate as a result of the animal movements and to compare different irradiation procedures with respect to variations in sampled integral-dose rate.**

NOMENCLATURE

Integral dose ϵ	Total electromagnetic energy absorbed by the test animal.
Integral-dose rate $\dot{\epsilon}$	The time rate of absorption of total electromagnetic energy.
Sampled integral-dose rate $\dot{\epsilon}_i^*$	The measured change in total electromagnetic energy absorbed during the ith time interval divided by the value of that interval.
Distributed dose D	The electromagnetic energy absorbed by a macroscopic element of mass within the test animal divided by the value of that mass.

Manuscript received May 28, 1974; revised August 27, 1974.
The authors are with the Division of Biological Effects, Bureau of Radiological Health, Food and Drug Administration, U. S. Department of Health, Education and Welfare, Rockville, Md. 20852.

INTRODUCTION

CURRENTLY, animals in microwave biological-effects experiments are irradiated by a variety of exposure-field configurations. Some of the irradiating apparatus include plane wave, focused field, aperture source, stripline, and waveguide. For some of these apparatus, the dosimetry is quantified in terms of external-field measurements using detectors that respond to the electric field squared. The results of the field measurements are presented in terms of power density (milliwatts/square centimeter) assuming a far-field relationship between the electric and magnetic fields. Biological effects, however, are related to the induced internal electromagnetic field in the biological body. It has been reported [1]–[3] that the induced electromagnetic field and hence the energy absorbed (proportional to the electric field squared) in a biological body depends on the size, geometry, and composition of the biological body. The energy absorption also depends on the type of exposure field, the source frequency [4]–[6], and the orientation of the biological body with respect to the exposure field. In an effort to quantify the microwave energy absorbed by small experimental animals, a waveguide system has been constructed and was reported previously [7]. The environmentally controlled microwave-waveguide irradiation facility operating at 2450 MHz allows for the measurement of the integral dose absorbed by a test animal during a given